

Review

A Review on Mesophase and Physical Properties of Cyclotriphosphazene Derivatives with Schiff Base Linkage

Zuhair Jamain ^{1,2,*} , Ahmad Nor Asyraf Azman ¹, Nurul Asma Razali ¹ and Mohamad Zul Hilmey Makmud ² 

¹ Organic Synthesis and Advanced Materials (OSAM) Research Group, Faculty of Science and Natural Resources, Universiti Malaysia Sabah, Jalan UMS, Kota Kinabalu 88400, Sabah, Malaysia

² Future Material and Sustainable Energy (FuSE) Research Group, Faculty of Science and Natural Resources, Universiti Malaysia Sabah, Jalan UMS, Kota Kinabalu 88400, Sabah, Malaysia

* Correspondence: zuhairjamain@ums.edu.my

Abstract: Over the last decades, liquid crystalline has been of great recent importance due to many unique and different features. The linking unit, terminal group, and core system are the most factors to influence the liquid crystal behaviour. Schiff base linkage with the formula of $-C=N-$ can maintain linearity by providing the stepped core structure with high stability. Incorporation of Schiff base linkage in cyclotriphosphazene system enhances the mesophase characteristic and high thermal stability. This review focussed on the mesophase behaviour and physical properties of cyclotriphosphazene derivatives attached to Schiff base linkages. A basic introduction to liquid crystalline materials, including description and classification, is provided in this review.

Keywords: liquid crystal; Schiff base; cyclotriphosphazene; core system; linking unit



Citation: Jamain, Z.; Azman, A.N.A.; Razali, N.A.; Makmud, M.Z.H. A Review on Mesophase and Physical Properties of Cyclotriphosphazene Derivatives with Schiff Base Linkage. *Crystals* **2022**, *12*, 1174. <https://doi.org/10.3390/cryst12081174>

Academic Editors: Doina Manaila-Maximean, Viorel Circu and Octavian Danila

Received: 9 July 2022

Accepted: 12 August 2022

Published: 21 August 2022

Publisher's Note: MDPI stays neutral with regard to jurisdictional claims in published maps and institutional affiliations.



Copyright: © 2022 by the authors. Licensee MDPI, Basel, Switzerland. This article is an open access article distributed under the terms and conditions of the Creative Commons Attribution (CC BY) license (<https://creativecommons.org/licenses/by/4.0/>).

1. Introduction

Liquid crystal is the middle stage of solid and liquid. The Austrian chemist and botanist, Friedrich Reinitzer discovered liquid crystals and noticed that cholesterol benzoate did not melt into a clear liquid but stayed cloudy [1]. The cloudy liquid became transparent upon further heating which formed the liquid crystalline state [2]. In the early stages of liquid crystal, it was known that an aliphatic chain fluid had to be one end of the terminal substituent bound to the molecular centre in order to dilute the central rigid organic core, creating a comparatively low melting point or at least a melting point low enough to exist for liquid crystalline property [3].

Molecules exhibit orientational and three-dimensional positional orders in the crystalline state [4]. In a three-dimensional lattice, the constituent molecules of strongly structured solids occupy specific locations and point their axes in fixed directions. In some situations, liquid crystal phases have orientational order (molecular propensity to point in a particular direction called director, n) and spatial order in one or two dimensions. On the other hand, the molecules move spontaneously in the isotropic liquid state and spin freely in all possible directions. In other words, the liquid crystal has movement and consistency like a liquid but may have a solid (crystal) alignment and positional order. Therefore, liquid crystals have been characterized as combining properties of both the crystalline and the liquid states [4].

The mesophases occurred in a certain temperature range. If the temperature is too high, the thermal motion will destroy the delicate ordering of the liquid crystal phase, pushing the material into the isotropic phase. If the temperature is too low, most liquid crystal materials will form a conventional crystal [5]. The molecular arrangement of these phases can be illustrated in Figure 1.

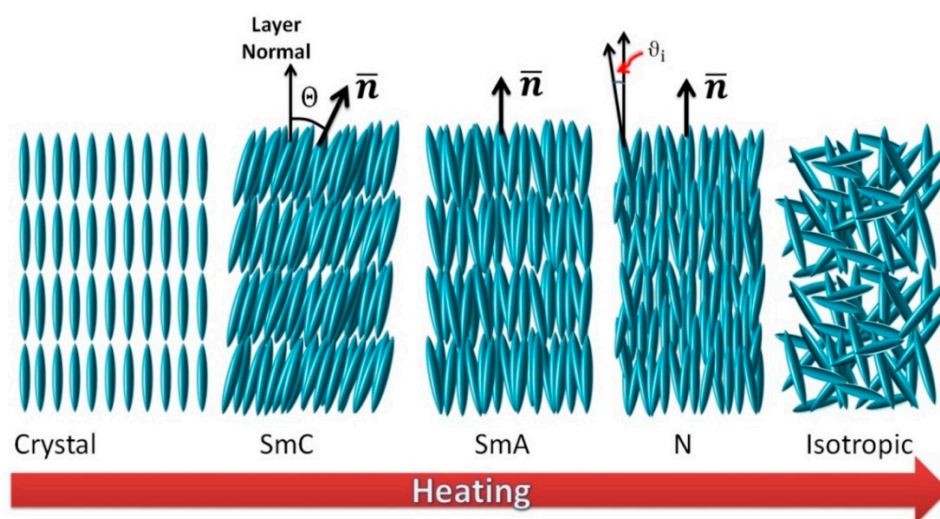


Figure 1. The molecular arrangement of crystal, liquid crystalline (SmC, SmA, and N) and isotropic phases. Reprinted/adapted with permission from Ref. [6]; published by MDPI AG, 2017.

1.1. Classification of Liquid Crystals

There are two classes of liquid crystals, which are thermotropic and lyotropic. Thermotropic liquid crystals are temperature dependent, whereas lyotropic liquid crystals are mainly solvent dependent [7]. Thermotropic liquid crystal displays mesomorphic behaviour within a specific temperature range [8].

1.1.1. Thermotropic Liquid Crystals

By simultaneous loss of the long-range positional and orientational orders, most of the heating crystals turn into the isotropic liquid phase. The melting point is considered the temperature at which the crystal turns into mesophase, while that from the mesophase to the isotropic state is called the clearance point. Materials possessing thermotropic liquid crystal properties are often chemical or organic materials containing metals. In defining the formation and type of the liquid crystalline phases, molecular form anisotropy plays a major role [9].

1.1.2. Types of Liquid Crystal Arrangement

There are four types of liquid crystal arrangement: nematic, smectic, cholesteric and columnar liquid crystals. Nematic liquid crystal is a molecular arrangement in the axial direction, smectic liquid crystal is the layered molecular arrangement, and layered molecular arrangement with spiral form is cholesteric liquid crystal [10].

Molecules in a nematic mesophase have an orientational order in the nematic (N) phase but no positional order and they are directed toward a specific direction named the director, n . Unit vector, n , represents the director orientation. The molecules can rotate along their long axis in a nematic, and their ends do not have a preferential structure, even though they vary. Anisotropic forms have molecules forming nematic crystalline mesophases, mostly with rigid molecular backbones that describe the long axes of molecules [11]. Liquid crystallinity is much more likely to happen if the molecules consist of flat segments in the structures. Strong dipole moments and readily polarizable groups are often included in liquid crystalline compounds [9].

The name cholesteric is of historical origin. The cholesteric mesophase is similar to the nematic, which has an orientational order. It differs from nematic mesophase, where the neighbouring molecules have a weak tendency to align at a slight angle with each other. It happens in situations where there are chiral constituent molecules [12]. There is a weak tendency for adjacent molecules to converge at a small angle with one another in these structures. This causes a helical structure with an axis perpendicular to the director. Depending on molecular conformation, the helical twist can be right-handed or left-handed.

The peculiar optical properties of the process, such as selective reflection, are responsible for that helical structure. The polarization plane is rotated along the direction of the helix as plane-polarized light interacts with this chiral macroscopic structure [13,14].

The molecular centre of gravity is organized in equidistant planes on average in certain stages, so that positional order is also present in addition to orientational order, contributing to a layered structure, these phases were called smectic. The stratification is the important characteristic of a smectic mesophase which distinguishes it from a nematic or cholesteric mesophase [15]. Smectic mesophases are categorized into various groups according to the chronological order of their identification, based on the molecular arrangements within the layer and the degree of inter-layer correlations. The smectic phases were classified with code letters A, B, C, D, and E. Furthermore, in contrast to the standard layer, these smectic liquid crystal phases can be divided into two groups based on whether or not the constituent molecules are tilted. The SmA, SmB and SmE phases are orthogonal, while SmC phases are tilted. Among the numerous smectic phases, SmA and SmC are the two most widely found and thoroughly studied [16].

Molecules are arranged in layers throughout the smectic A (SmA) phases and the movement of molecules from one layer to another is minimal. The molecules in SmA are positioned with long axes parallel to the layer normal [17]. The phase of smectic C (SmC) varies from the phase of SmA in terms of molecular structure in which the molecules in the phase of SmC are angled uniformly at an angle, as opposed to the normal layer, z [16]. The nematic mesophase often happens at a higher temperature than the smectic. As the temperature falls, the smectic mesophases occur from SmA \rightarrow SmC \rightarrow SmB [9].

Columnar liquid crystal is formed by flat-shaped molecules containing a central atomic core with different terminal groups, such as an aliphatic chain [18]. This type of liquid crystal was originally known as discotic liquid crystal since the columnar structure comprises disk-like molecules assembled into a cylindrical structure [9]. The flat-shaped disk is organized into columns by nature, caused by the strong π - π stacking interaction along the disk-like core [19]. Columnar liquid crystal is grouped based on the molecular packing of the molecule. It exhibits 3D fluid nematic and columnar phases where the molecular disk mount on top of each other to form 1D columns [20,21]. The nematic and columnar phases are in a dynamic state of ordered molecular aggregation, with nematic being the most mobile mesophase [22].

The most widely used instrument for distinguishing the phases of liquid crystals is the polarizing optical microscope (POM), which shows a mesophase's distinctive optical structure. The optical patterns are normally observed between two glass plates in thin layers of the sample, chemically treated for either homogeneous or homeotropic arrangement of the molecules. Liquid crystals form into various mesophase systems depending on the strength of intra and intermolecular interactions, and they also display their corresponding polarized optical microscopy (POM) textures for each phase, such as schlieren texture of nematic, fingerprint texture of cholesteric, and fan-shaped focal conic texture of smectic liquid crystal.

2. Linking Unit

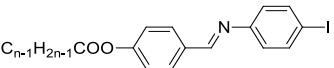
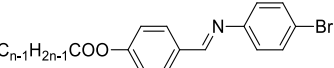
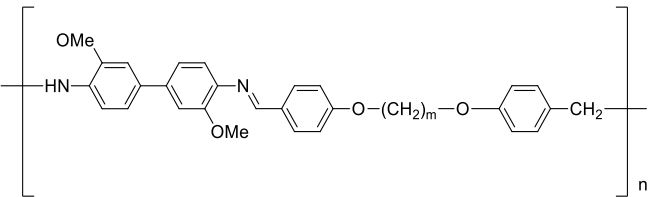
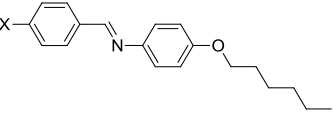
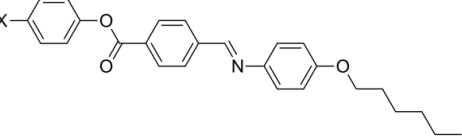
A mesogenic molecule is made up of the core, lateral substituents, and terminal chains. The core provides the rigidity required for anisotropy, while the terminal chains offer stability to maintain the mesophase molecular alignment [16]. The core is normally an aromatic ring that is linearly linked. The rings may be linked directly to each other, or they might have been joined by linking units such as $-\text{CH}=\text{CH}-$, $-\text{CH}=\text{N}-$, $-\text{NH}-\text{CO}-$, and $-\text{COO}-$. The terminal chains are straight alkyl or alkoxy chains, but a polar substituent is often one of the terminal units. Depending on the type of substituents and their compositions, the calamitic molecules form either nematic or smectic mesophases [23].

2.1. Azomethine Linkage (Schiff Base)

Schiff base is a compound containing an imine or azomethine functional groups. Hugo Schiff first discovered Schiff base through the condensation process of primary amines with a carbonyl compound, resulting in the formation of secondary aldimine moieties $R-CH=N-R$ [20,24]. Schiff base is a crucial group of compounds as it possesses a variety of applications in many fields of study, including medicinal and pharmaceutical. It is also used widely as a catalyst, stabilizer, and corrosion inhibitor [24].

The linking units such as Schiff base are usually conjugated with benzene rings to elongate and enhance the compound's polarizability to enhance the liquid crystal behaviour. The Schiff base linkage offers a stepped core structure that can keep the molecules' linearity and offer great stability. Due to this, mesophase development is induced, and the connecting group often controls the phase transition temperatures and the physical characteristics [9,10]. The example of Schiff base compounds that exhibited the liquid crystalline properties are shown in Table 1.

Table 1. Schiff base compounds attached to different terminal ends.

Structure of Compound	Terminal Group	Ref.
	$n = 4$ (1a); 6 (1b); 8 (1c); 10 (1d); 12 (8e); 14 (1f)	[25]
	$n = 8$ (2a); 10 (2b); 12 (2c); 14 (2d); 16 (2e); 18 (2f)	[26]
	$m1 = 6$; $m2 = 9$	[27]
	X = Me ₂ N (5a); MeO (5b); H (5c); Cl (5d); F (5e); CN (5f); NO ₂ (5g)	[28]
	X = CH(CH ₃) ₂ (7a); H (7b); I (7c); F (7d)	[29]

2.2. Liquid Crystalline Properties of Compounds

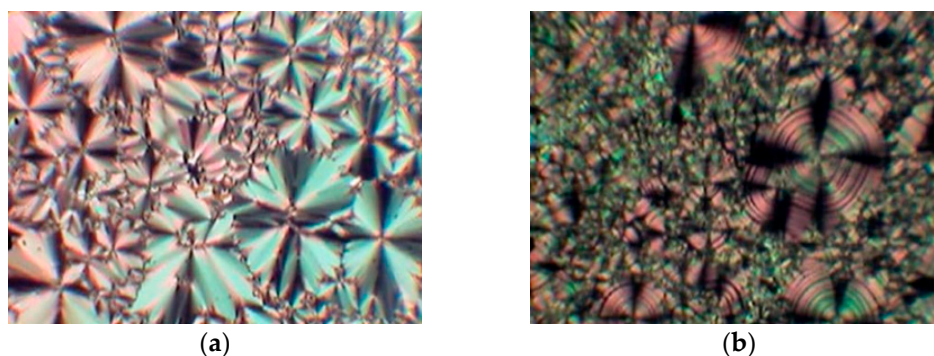
Ha et al. (2011) synthesized 4-iodoaniline that was condensed with 4-hydroxybenzaldehyde and then refluxed in methanol for an hour to yield azomethine compounds, compounds 1(a–f) [25]. All the crude was purified by repeated recrystallization using ethanol and hexane until constant melting points were obtained. Using a differential scanning calorimeter, transition temperatures and enthalpy variations were calculated. The study findings are found in Table 2.

Table 2. Phase transition temperatures of compound **1(a–f)**. Reprinted/adapted with permission from Ref. [25]; published by Elsevier, 2011.

Compound	Temperature (°C)	Transitions	ΔH kJ/mol
1a	116.1	Cr \rightarrow I	29.9
	112.1	I \rightarrow Cr	29.6
1b	101.3	Cr \rightarrow SmA	52.2
	111.1	SmA \rightarrow I	10.4
	104.3	I \rightarrow SmA	23.1
	31.4	SmA \rightarrow Cr	36.6
1c	86.6	Cr \rightarrow SmA	57.9
	115.3	SmA \rightarrow I	10.4
	107.8	I \rightarrow SmA	7.0
	36.4	SmA \rightarrow Cr	43.6
1d	86.6	Cr \rightarrow SmA	61.6
	115.7	SmA \rightarrow I	6.4
	108.3	I \rightarrow SmA	5.8
	27.5	SmA \rightarrow Cr	38.7
1e	101.6	Cr \rightarrow SmA	78.2
	109.6	SmA \rightarrow I	11.7
	102.0	I \rightarrow SmA	23.9
	84.3	SmA \rightarrow Cr	70.2
1f	94.3	Cr \rightarrow SmA	70.5
	116.5	SmA \rightarrow I	16.2
	110.1	I \rightarrow SmA	16.3
	61.6	SmA \rightarrow Cr	74.3

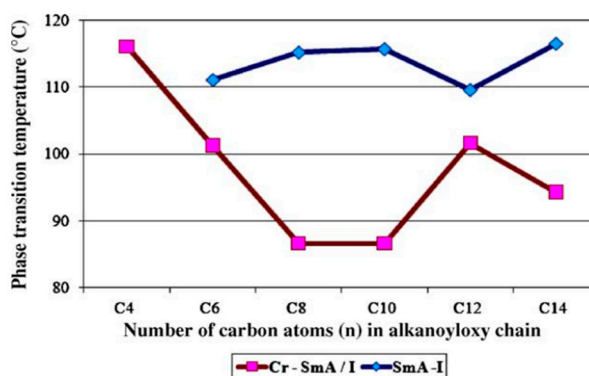
Note: Cr = crystal; SmA = smectic A; I = isotropic.

Liquid crystalline textures were identified under a polarizing optical microscope equipped with a hot stage and temperature regulator. By comparing the observed textures with those recorded in the literature, phase identification was made [30,31]. Both compounds displayed fan-shaped textured enantiotropic smectic A step with the exception of n-butanoyloxy derivative. The fan-shaped texture in Figure 2a with the smectic A phase was first observed after cooling of **1e** from isotropic liquid, accompanied by coexisting planar and homeotropic regions of the SmE phase as shown in Figure 2b.

**Figure 2.** The optical photomicrograph of compound **1e** with (a) SmA and (b) SmE phase textures. Reprinted/adapted with permission from Ref. [25]; published by Elsevier, 2011.

The process shifted from non-mesogenic to enantiotropic smectic phase A with the increasing length of the terminal chain [23]. For the n-butanoyloxy derivative to be mesogenic, the molecule is too stiff. The homologous members demonstrated enantiotropic smectic

step A from n-hexanoyloxy to n-tetradecanoyloxy derivatives. The spectrum of smectic phase A from n-hexanoyloxy to n-decanoyloxy members is obvious from Figure 3. This is because the rise in terminal alkanoyloxy side chain contributed to the smectic properties being enhanced. However, due to mesogenic core dilution, the spectrum of the smectic A phase of n-dodecanoyloxy and n-tetradecanoyloxy decreased [32,33].



Comp	1a	1b	1c	1d	1e	1f
<i>n</i>	4	6	8	10	12	14

Figure 3. A plot of phase transition temperatures against a number of carbon atoms (*n*) in the alkanoyloxy chain. Reprinted/adapted with permission from Ref. [25]; published by Elsevier, 2011.

In 2012, Ha et al., synthesized azomethine liquid crystals with different terminal chain lengths. The results showed that n-octanoyloxy exhibits enantiotropic smectic A and smectic B phases in n-dodecanoyloxy derivatives, while n-tetradecanoyloxy showed enantiotropic smectic A and monotropic B phases in n-octadecanoyloxy derivatives. Table 3 summarizes the findings.

Table 3. Phase transition of compound 2(a–f). Reprinted/adapted with permission from Ref. [26]; published by Elsevier, 2012.

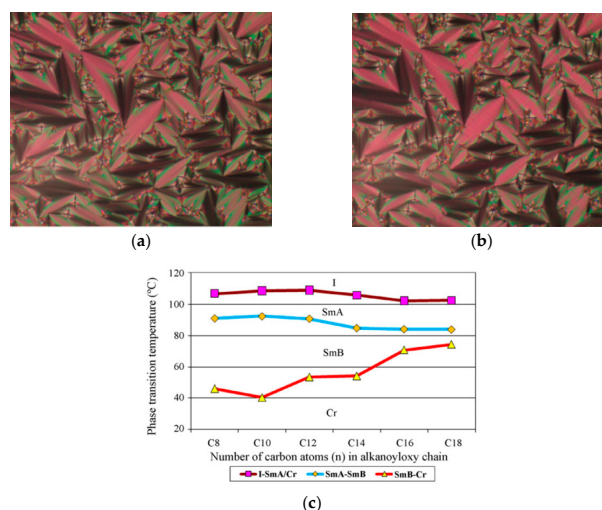
Compound	Temperature (°C)	Transitions	ΔH kJ/mol
2a	89.62	Cr → SmB	25.09
	94.40	SmB → SmA	2.27
	110.55	SmA → I	6.39
	106.78	I → SmA	6.53
	91.03	SmA → SmB	3.02
	46.16	SmB → Cr	10.64
2b	86.70	Cr → SmB	26.28
	96.17	SmB → SmA	2.78
	113.55	SmA → I	8.16
	108.44	I → SmA	8.65
	92.33	SmA → SmB	3.27
	40.48	SmB → Cr	28.73
2c	90.95	Cr → SmB	31.54
	96.50	SmB → SmA	3.09
	115.08	SmA → I	8.16
	108.82	I → SmA	7.46
	90.83	SmA → SmB	3.20
	53.47	SmB → Cr	31.75

Table 3. Cont.

Compound	Temperature (°C)	Transitions	ΔH kJ/mol
2d	91.26	Cr \rightarrow SmA	41.08
	110.55	SmA \rightarrow I	8.08
	105.72	I \rightarrow SmA	8.00
	84.83	SmA \rightarrow SmB	3.25
	54.15	SmB \rightarrow Cr	36.98
2e	94.35	Cr \rightarrow SmA	53.70
	107.13	SmA \rightarrow I	9.27
	102.16	I \rightarrow SmA	10.45
	84.13	SmA \rightarrow SmB	3.79
2f	70.74	SmB \rightarrow Cr	50.79
	97.11	Cr \rightarrow SmA	73.88
	105.50	SmA \rightarrow I	11.44
	102.39	I \rightarrow SmA	11.93
	83.92	SmA \rightarrow SmB	4.52
	74.26	SmB \rightarrow Cr	69.16

Note: Cr = crystal; SmB = smectic B; SmA = smectic A; I = isotropic.

For enantiotropic materials, during heating and cooling processes, similar mesophases were observed. The homogeneous focal-conic texture of the smectic A phase after cooling compound **2a** from isotropic liquid was first observed in Figure 4a, accompanied by temporary transition bars showing the transition phase from smectic A to smectic B phase, Figure 4b. Figure 4c displays a plot of phase transition temperatures against the number of carbon atoms (n) in the alkanoyloxy chain during the cooling scan. It can be deduced that the length of the terminal alkanoyloxy chains affected the mesomorphic properties based on the plot [31]. The phase shifted from enantiotropic to monotropic smectic phase B with the increasing length of the terminal chain. It is evident from the graph that the spectrum of mesophase increases from n-octanoyloxy to n-decanoyloxy members. Due to the rise in terminal alkanoyloxy chain length, this phenomenon has contributed to the improvement of smectic properties. However, owing to the dilution of the mesogenic core, the mesophase spectrum of n-dodecanoyloxy to n-octadecanoyloxy decreased [26]. The optimal exhibition (largest mesophase range) in both smectic phase A and smectic phase B was shown by n-decanoyloxy derivatives.



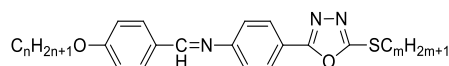
Comp	2a	2b	2c	2d	2e	2f
n	8	10	12	14	16	18

Figure 4. The optical photomicrograph of compound **2a**, (a) temporary transition bars, (b) from smectic A to smectic B phase, and (c) plot of phase transition temperatures. Reprinted/adapted with permission from Ref. [26]; published by Elsevier, 2012.

In 2012, Kostromin et al., reported the synthesis of 1,6-bis (formylphenoxy) hexane or 1,9-bis (formylphenoxy) nonane by polycondensation of equimolar amounts of *o*-dianisidine with 1,6-bis (formylphenoxy) hexane or 1,9-bis (formylphenoxy) nonane in spacers of thermotropic polyazomethines **m1** and **m2** having 6 and 9 methylene groups, respectively, in spacers [27].

In this study, **m1** displays an extreme endothermic peak at 111 °C after the first heating scan leading to the Cr-LC phase change, followed by a smaller endothermic peak at 154 °C, which is due to the LC-N transition phase. The glass transformation can be quickly detected at 33 °C during the second heating scan. While, **m2** reveals an extreme endothermic peak at 33 °C attributable to enthalpy relaxation in the solid phase during the first heating scan, followed by a rather slight endothermic peak at around 60 °C, which is due to the Cr-LC phase shift.

Naser et al. (2014) synthesized by dissolving 1-(4-alkoxybenzylidene amino)-4-(2-*n*-hexylthio-1,3,4-oxadiazole-5-yl) benzene **3(a–f)** and **4(a–f)** of 2-*n*-hexyl thio-5-(4-aminophenyl)-1,3,4-oxadiazole in absolute ethanol with 4-*n*-hexaloxo- or heptaloxo-benzaldehyde and glacial acetic acid [34]. The mixture will be refluxed for 3 h, evaporated the solvent, crystallized the petroleum ether residual, and then accumulated yellow products.



Comp	3a	3b	3c	3d	3e	3f
m	6	6	6	6	6	6
<i>n</i>	3	4	5	6	7	8
Comp	4a	4b	4c	4d	4e	4f
m	7	7	7	7	7	7
<i>n</i>	3	4	5	6	7	8

All the compounds have mesomorphic properties in both compounds **3(a–f)** and **4(a–f)** sequence. Smectic A (SmA), smectic C (SmC) and/or nematic (N) phases of enantiotropic dimorphism exist in all members of those two series. The homologous **3a**, **3b** and **3c** have a dimorphism, nematic and smectic A (SmA) mesophase activity for the series of compound **3**. Compounds **3d** and **3e** show enantiotropic smectic A and C (SmA and SmC) and the last homologue, compound **3f** demonstrates pure smectic C (SmC) mesophase. All compounds **4(a–f)** also demonstrated mesomorphic. Compounds **4a**, **4b**, **4c** and **4d** illustrated the behaviour of dimorphism, nematic and smectic A (SmA) mesophases. The last two homologues, compounds **4e** and **4f** demonstrated the purely Smectogenes SmA and SmC mesophases of dimorphism. Table 4 showed the transition phase and thermodynamic data for such substances.

Table 4. Phase transition temperature. Reprinted/adapted with permission from Ref. [34]; published by JIARM, 2014.

Compound	Temperature (°C)	Transitions	ΔH kJ/mol	ΔS kJ/K mol
3a	67	Cr → Cr	—	—
	100	Cr → SmA	24.74	0.25
	122	SmA → N	—	—
	200	N → I	—	—
3b	95	Cr → SmA	65.54	0.69
	110	SmA → N	—	—
	226	N → I	28.51	0.13

Table 4. Cont.

Compound	Temperature (°C)	Transitions	ΔH kJ/mol	ΔS kJ/K mol
3c	94	Cr \rightarrow SmA	37.00	0.40
	121	SmA \rightarrow N	0.51	0.01
	136	N \rightarrow I	0.92	0.01
3d	83	Cr \rightarrow SmC	31.91	0.39
	120	SmC \rightarrow SmA	—	—
	137	SmA \rightarrow I	1.90	0.02
3e	89	Cr \rightarrow SmC	32.37	0.36
	110	SmC \rightarrow SmA	—	—
	143	SmA \rightarrow I	3.75	0.03
3f	78	Cr \rightarrow SmC	32.12	0.41
	146	SmC \rightarrow I	3.29	0.02
4a	80	Cr \rightarrow SmA	28.93	0.36
	111	SmA \rightarrow N	—	—
	134	N \rightarrow I	1.46	0.01
4b	81	Cr \rightarrow SmA	29.61	0.36
	125	SmA \rightarrow N	0.43	0.03
	136	N \rightarrow I	0.49	0.04
4c	84	Cr \rightarrow SmA	20.47	0.24
	123	SmA \rightarrow N	—	—
	134	N \rightarrow I	0.93	0.01
4d	86	Cr \rightarrow SmA	23.47	0.27
	120	SmA \rightarrow N	—	—
	135	N \rightarrow I	1.75	0.01
4e	71	Cr \rightarrow SmC	27.41	0.38
	138	SmC \rightarrow SmA	2.73	0.02
	164	SmA \rightarrow I	0.86	0.01
4f	64	Cr \rightarrow SmC	25.94	0.41
	112	SmC \rightarrow SmA	—	—
	143	SmA \rightarrow I	4.26	0.03

Note: Cr = crystal; SmC = smectic C; SmA = smectic A; N = nematic; I = isotropic.

Figure 5 displays a plot of transition temperatures against the number of carbon atoms in the lateral alkoxy chain. The presence of nematic and smectic SmA phase transitions in both heating and cooling processes was shown by compounds 3a to 3c and 4a to 4d.

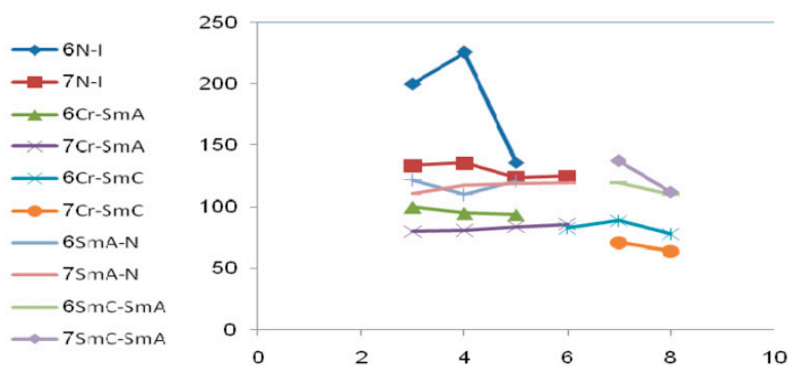


Figure 5. Graph of transition temperature against the number of carbon atoms. Reprinted/adapted with permission from Ref. [34]; published by JIARM, 2014.

Compound 4c provided the distinctive SmA texture of the focal conic texture on the heating cycle and nematic Schlieren textures from 84 to 134 °C when isotropization occurred. Nematic droplets unified into an expanded Schlieren texture with distinctive two-

and four-brush singularities were observed during cooling [34]. Compound **4c** is similar to the behaviour of other compounds in both series. The SmA process was distinguished by the development of the usual focal-conic fan texture of the sequence of compounds **3(a–f)** and **4(a–f)**. A bottonite texture characteristic of the SmA was observed while cooling from the isotropic material, converting the texture to the fan-shaped texture coexisting with spherulitic areas. Compounds **3d** to **3f** and **4e** and **4f** showed the enantiotropic phases of SmA and SmC. An orthogonal fan texture typical of the SmA was observed when cooling slowly from the isotropic fluid. A fan-shaped texture coexisting with spherulitic regions displayed the SmA process present in these compounds. A stage defined by its distinctive Schlieren textures forms when further cooling of the SmA texture transition to SmC.

Nafee et al. (2020) used two methods to synthesise N-arylidene-4-(hexyloxy) benzenamines, **5(a–g)**, the first approach being the traditional method for two hours under reflux conditions in ethanol [28]. Data in Figure 6 showed that except for the **5c** (X=H) and **5g** (X=NO₂) compounds, the analogous derivatives **5(a–g)** are mesomorphic. Compound **5b** analogue is dimorphic for electron-donating groups, displaying monotropically smectic A (SmA) and nematic phases (N), whereas compound **5b** (X=OCH₃) is solely nematogenic, displaying only a monotropic nematic phase with a limited stability spectrum, as seen in Figure 7 [28]. Cl substituted compound (**5d**) reported dimorphic phases displaying smectic A and nematic mesophases during heating and cooling. CN derivative (**5f**) is strictly smectogenic with enantiotropic SmA phase, whereas **5e** analogues (F-substituent) are monomorphic with monotropic SmA phase.

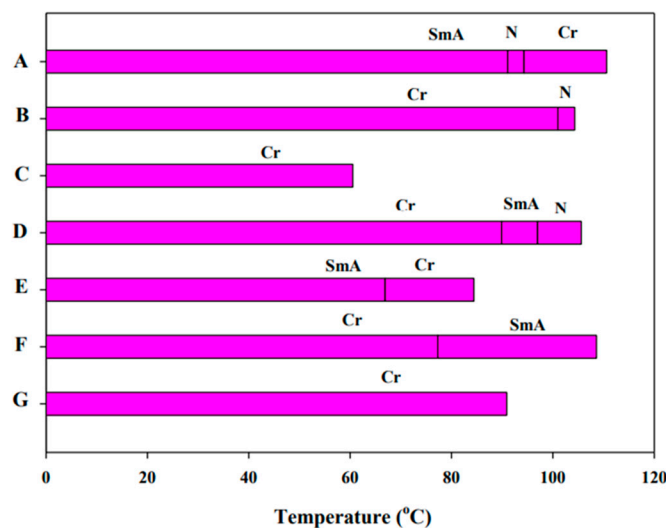


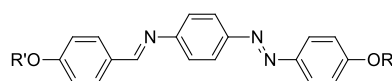
Figure 6. DSC transition of **5(a–g)**. Reprinted/adapted with permission from Ref. [28]; published by Elsevier, 2020.



Figure 7. The optical photomicrograph of (a) nematic phase of compound **5b** at 99.0 °C upon cooling; (b) Smectic A phase of compound **5f** at 106.0 °C. Reprinted/adapted with permission from Ref. [28]; published by Elsevier, 2020.

Naoum et al. (2015) stated that the stability and styles of mesophase development rely primarily on the dipole moment of the mesogenic portion of the molecule that depends on the terminal polar group attached and the steric one that differs according to the substituent location and length [35]. The addition of a substituent into the terminal position of a liquid crystalline compound will have two opposite effects: a reduction in mesophase stability due to the terminal group's steric effect and a rise or reduction in its polarity anisotropy due to its polarizing effect molecule [36]. In addition, it is obvious that terminal groups play an important role in affecting the melting point of the products prepared. The terminal substituent (X) in the molecules can be located as $CN > Cl > CH_3O > N(CH_3)_2 > F > H \approx NO_2$ in order to improve mesophase stability. The order of improvement of the mesophase spectrum, however, is as follows: $CN > N(CH_3)_2 > F > Cl > CH_3O > H \approx NO_2$.

Jamain et al. (2019) reported the synthesis of (4-heptyloxybenzylidene)-[4-(4-pentyloxyphenylazo)-phenyl]-amine-4-(4-pentyloxy-phenylazo)-phenylamine and 4-heptyloxybenzaldehyde to yield compounds **6(a–f)** [37].



Comp	6a	6b	6c	6d	6e	6f
R'	C ₇ H ₁₅	C ₁₂ H ₂₅	C ₇ H ₁₅	C ₁₂ H ₂₅	C ₇ H ₁₅	C ₁₂ H ₂₅
R	C ₅ H ₁₁	C ₅ H ₁₁	C ₉ H ₁₉	C ₉ H ₁₉	C ₁₂ H ₂₅	C ₁₂ H ₂₅

From both heating and cooling cycles, compound **6a** did not display any liquid crystal phase. Compounds **6(b–d)** display phase transition from crystal to smectic A and nematic phases before reaching the heating period isotropic phase. Compound **6e** demonstrated smectic C phase and compound **6f** in both cycles displayed smectic. Figure 8 illustrates the mesophase textures for compounds **6b**.

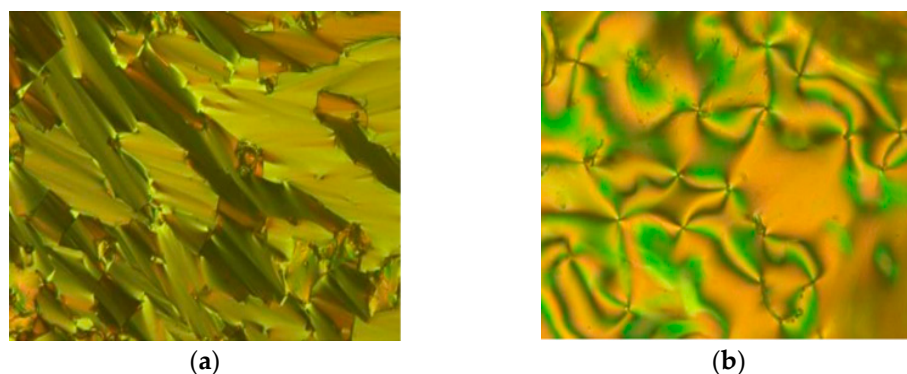


Figure 8. The optical photomicrograph of compound **6b**; (a) SmA at 126.21 °C; (b) nematic at 212.45 °C. Reprinted/adapted with permission from Ref. [37]; published by Malaysian Institute of Chemistry, 2019.

Overall, the length of the alkoxy chain influenced the mesogenic properties. Melting temperatures and clearing temperatures are lowered by increasing the number of carbon chains. As the molecule's flexibility improved, the terminal attraction became smaller, leading to lower phase stability [37,38]. In general, compounds with long alkyl chain lengths displayed enantiotropic mesophase that is thermodynamically stable, whereas compounds with shorter alkyl chains showed monotropic mesophase as these compounds had unpredictable behaviour [39]. Consequently, compound **6a** with a shorter alkyl chain was unable to cause the development of mesophase. Smectic phase formation may be due to the lamellar packing. The layered system broke down at the definite temperature and the magnitudes of the end-to-end side intermolecular attractions and the ideal permanent dipole moment were still preserved. This prompted the homologue to adopt a nematogenic

character in parallel orientational order, either directly or by a smectic process in an enantiotropic fashion [40,41].

Hagar et al. (2019) synthesized liquid crystal compounds by dissolving molar equivalents of 4-[(4-(hexyloxy)phenylimino)methyl] benzoic acid and 4-substitutedphenol into dry methylene chloride [29].

Figure 9 indicates enantiotropic mesomorphics with broad stability for all the compounds. Compounds **7(a–d)**, the current mesomorphic substances, are solely smectogenic, showing a process of monomorphic smectic A (SmA). Compound **7c** (X = I), however, is dimorphic and exhibits phases SmA and N. Compound **7a** which is substituent for $\text{CH}(\text{CH}_3)_2$, exhibits a SmA phase with a thermal stability range of 24.1 °C, while the unsubstituted derivative **7b** has a smectic phase with a temperature range of 20.1 °C and a low melting temperature of 67.3 °C. Gulbas et al. (2014) reported that the mesomeric part of the molecule's dipole moment influences the form and stability of the formed mesophase, which depends on the terminal polar substituent attached and the steric one that varies according to size [42]. The halogen substituent showed a clear effect on the mesomorphic activity of the Schiff base molecules at the terminal location [43]. Dimorphic, with the greatest thermal nematic stability (182.0 °C) and SmA stability (136.3 °C), is the halogenated compound **7c** (X = I). The transition melting temperature of compound **7c** is 75.4 °C and the ranges of its smectic and nematic phases are 60.9 and 45.7 °C. The fluoro substituted derivative **7d** is monomorphic smectogenic, with a broad thermal stability SmA range (73.4 °C) lower than the thermal stability C range. The terminal substituent (X) in the molecules may be arranged in accordance with their capacity to increase the range and stability of the mesophase.

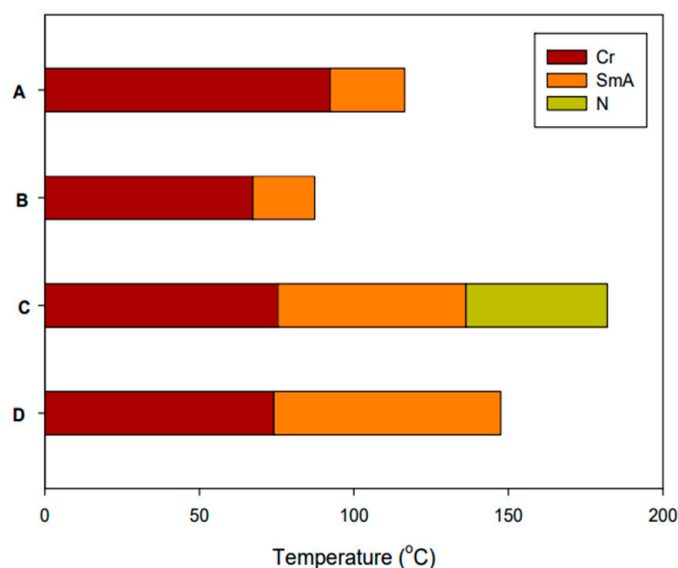


Figure 9. DSC transition of compound **7(a–d)**. Reprinted/adapted with permission from Ref. [29]; published by MDPI AG, 2019.

In deciding the form and stability of the improved mesophase, a competitive relationship between end-to-end intermolecular aggregation and side-side parallel interaction plays an important role. For the prepared substances, the types of mesophase textures observed were described and depicted in Figure 10.



Figure 10. The optical photomicrograph for (a) the nematic phase of acid at 262.0 °C and (b) the smectic A phase of compound **7d** at 120.0 °C. Reprinted/adapted with permission from Ref. [29]; published by MDPI AG, 2019.

It was observed that the thermal stability of compound **E** is comparatively higher than that of its isomers **B** and **F** because of the contrast with their mesophase stability. In the location and inversion of the ester relation and the exchange in the place of terminal substituents, isomer **E** differs from prepared isomer **B**. Thus, the addition of a hexyloxy chain to the terminal ring, which is attached to the ester group rather than the mesogen (-CH=N-), tends to increase polarizability and thus strengthen the terminal intermolecular interaction between molecules, indicating a nematic process. The findings confirmed that, relative to the chains attached to the azomethine ligand, the influence of the alkoxy chain attached to the ester bond is more successful in the form and stability of phases [29].

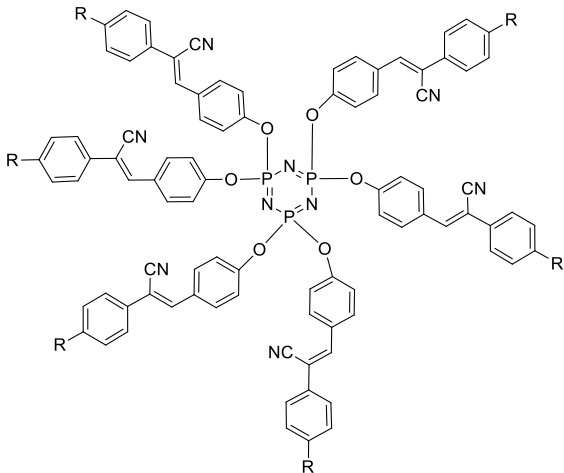
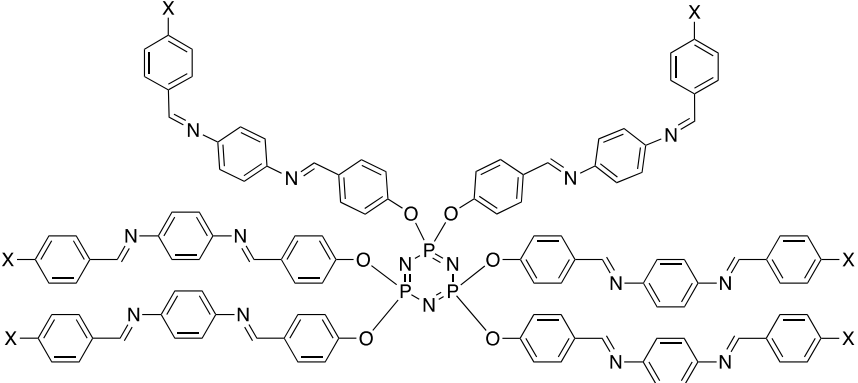
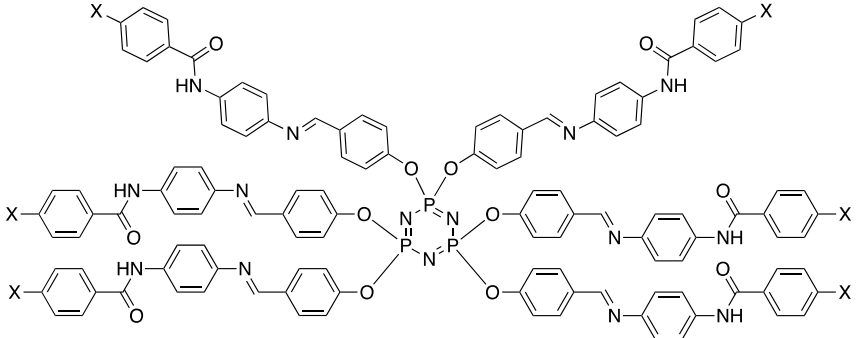
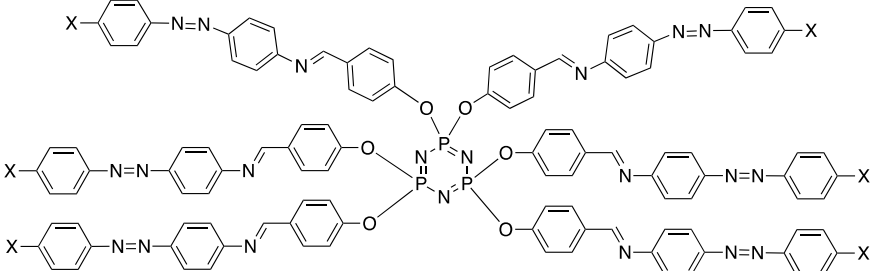
2.3. Liquid Crystalline Cyclotriphosphazene Derivatives

The hexa-functionality of cyclotriphosphazene system induces the exploration of liquid crystal study. Due to the presence of a chlorine atom in cyclotriphosphazene molecules, this atom can be substituted with any organic side arms [39]. The structure of cyclotriphosphazene bearing different organic side arms is illustrated in Table 5.

Table 5. Cyclotriphosphazene compounds bearing different terminal side arms.

Structure of Compound	Terminal Group	Ref.
	$R = \text{OC}_n\text{H}_{2n+1}$ Where $n = 6$ (8a); 10 (8b); 12 (8c)	[44]

Table 5. Cont.

Structure of Compound	Terminal Group	Ref.
	<p>R = OC_nH_{2n + 1} Where n = 4 (9a); 8 (9b); 12 (9c); 16 (9d)</p>	[45]
	<p>X = OC₇H₁₅ (10a); OC₉H₁₉ (10b); OC₁₀H₂₁ (10c); OC₁₂H₂₅ (10d); OC₁₄H₂₉ (10e); OH (10f); COOH (10g); Cl (10h); NO₂ (10i); NH₂ (10j)</p>	[46]
	<p>X = OC₇H₁₅ (11a); OC₉H₁₉ (11b); OC₁₀H₂₁ (11c); OC₁₂H₂₅ (11d); OC₁₄H₂₉ (11e); OH (11f); COOH (11g); Cl (11h); NO₂ (11i); NH₂ (11j)</p>	[47]
	<p>X = OC₇H₁₅ (12a); OC₉H₁₉ (12b); OC₁₀H₂₁ (12c); OC₁₂H₂₅ (12d); OC₁₄H₂₉ (12e); OH (12f); COOH (12g); Cl (12h); NO₂ (12i); NH₂ (12j)</p>	[48]

The incorporation of amide groups **8(a–c)** was carried out by Barbera et al. (2006) to increase the intermolecular forces between the cyclotriphosphazenes by hydrogen bonding [44]. As extracted from the thermogravimetric curves, these cyclotriphosphazenes

exhibit high thermal stability. In an inert atmosphere, the compounds are heat resistant up to a temperature close to 325 °C and display a sharp thermal decomposition at a maximum temperature degradation of about 370 °C. In addition, the existence of volatiles is ruled out based on curves of weight loss. Organophosphazenes are well known for their high thermal stability and have made these inorganic dendritic scaffolds ideal candidates for preparing thermally stable dendritic materials. The mesomorphic behaviour of these compounds, acquired as powdery samples, depends heavily on the length of the alkyl terminal chains. Cyclophosphazene containing hexyloxy chains was obtained as a glass material that followed a cold crystallization when heated and eventually melted to give a mesomorphic material at approximately 130 °C. Due to the high viscosity of the cyclotriphosphazene, this mesophase was hard to detect on this first heating run. However, a well-defined pseudo focal-conic fan-shaped texture along with homeotropic regions was clearly observed by POM cooling from the isotropic state [44].

The analysis also reveals the effect of the length of the alkyl chains in the packing of unconventional mesogens of this kind. The findings indicate a sluggish propensity to crystallize and this was further confirmed when a sample of this compound was recycled for 1 h at 110 °C. In this scan, an endothermic peak was observed at about 70 °C, accompanied by two small endothermic peaks at about 85 and 135 °C. In the cooling process, a better characterization was obtained. An isotropic phase-mesophase transformation was observed at around 135 °C, both via POM and DSC. The textures were specifically assigned to a Colh mesophase and showed a spontaneous propensity to homeotropic orientation. At around this temperature, the homeotropic regions modified and exhibited a mild birefringence. However, it is not possible to unambiguously assign the essence of this columnar mesophase. At temperatures below room temperature, the compound gradually crystallized and the melting transition was detected at around 5 °C. The presence of a great number of aliphatic chains allows a discotic form to be followed by the molecules and favours grouping into columns.

Bao et al. (2010) reported hexachlorocyclotriphosphazene (HCCP) attached to a different number of alkyl chains at the side arm [45]. Differential scanning calorimetry analyzed the thermal behaviours of compounds **9(a–d)**. Figure 11 displays the representative polarized optical micrographs (POM) of compounds **9(a–d)**. Compound **9a** demonstrated three heating transitions and two cooling transitions. The transition of heating and cooling on the DSC outcomes over a temperature range of 25–180 °C was observed for compound **9c**. On cooling, compound **9c** did not crystallize and displayed a wide temperature spectrum of liquid crystalline properties. This is possibly attributed to the combined influence of the rigid groups and the flexible chains that stopped compound **9c** from crystallizing. For terminal alkyl chains, the clearing temperatures of **9(a–d)** rose marginally. The temperatures of the melting transitions increased with terminal alkyl chains in addition to compound **9c**. For terminal chains, the transformations of enthalpies varied irregularly. Compounds **9(a–d)** of varying terminal alkyl chains have demonstrated different mesogenic cooling area lengths. As seen in Figure 11a, the usual threadlike texture was observed for **9a**. The characteristic schlieren textures that lead to the nematic process were observed for **9(b–d)** as shown in Figure 11b–d [45].

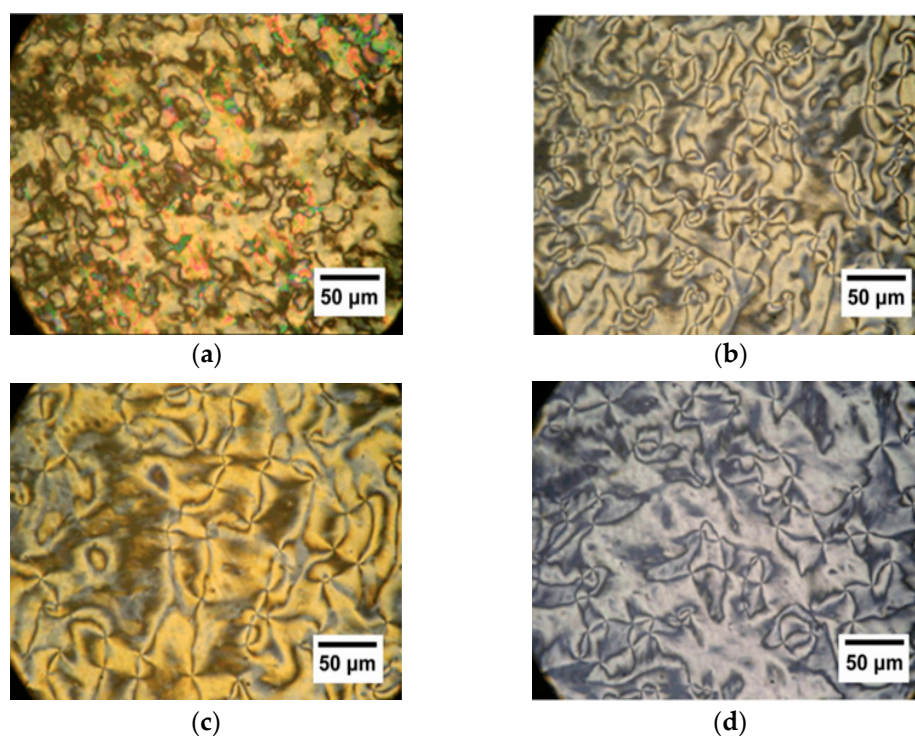


Figure 11. The optical photomicrograph of (a) **9a** at 150 °C, (b) **9b** at 155 °C, (c) **9c** at 160 °C and (d) **9d** at 166 °C. Reprinted/adapted with permission from Ref. [45]; published by Elsevier, 2010.

Jamain et al. (2020) synthesized cyclotriphosphazene derivatives **10(a–j)** with two Schiff base linking units having different terminal lengths [46]. In order to exhibit liquid crystal mesophase, a compound must have certain specifications. The key parameters for the liquid crystal behaviour of a molecule include the relatively thin or smooth molecular structure, typically centred on benzene rings [37,49]. In supplying rigidity to the molecules, aromatic ring cores linked directly or by linking units were very helpful [50]. In various molecules, terminal substituents can both attract and repel each other and control the aromatic rings' polarizability to which they are bound [51,52]. Alkyl side chain length was also shown to have a major impact on mesophase formation [53]. Increased aliphatic side chains in the liquid phase resulted in a higher organization, which in turn provides wider mesophases of liquid crystal. As a result, all the derivatives with alkoxy terminal chains **10(a–e)** showed the transition of mesophases. These compounds showed the SmA phase in both cycles. Interestingly, compounds **10a** and **10e** showed the extra mesophase transition of nematic and SmC, respectively. The formation of nematic was not favoured as the number of alkoxy chains increased due to an increase in the Van der Waals interactions. Meanwhile, compound **10e** adopted the SmC due to the stacking in the molecular arrangement. In addition, compounds **10(f–i)** with a small terminal group exhibited the nematic phases, due to the high polarity.

In the same year, Jamain and his coworkers were involved in the preparation of cyclotriphosphazene compounds with Schiff base and amide linkage [47]. Only **11(a–e)** compounds with Schiff base and amide linking units connected at the terminal end to varying chain lengths were found to be mesogenic. As seen in Figure 12, these compounds displayed a Smectic A (SmA) stage of focal-conic fans in both heating and cooling stages. The phase transition from crystal to isotropic in the heating cycle was only seen by compounds **11(f–j)**.

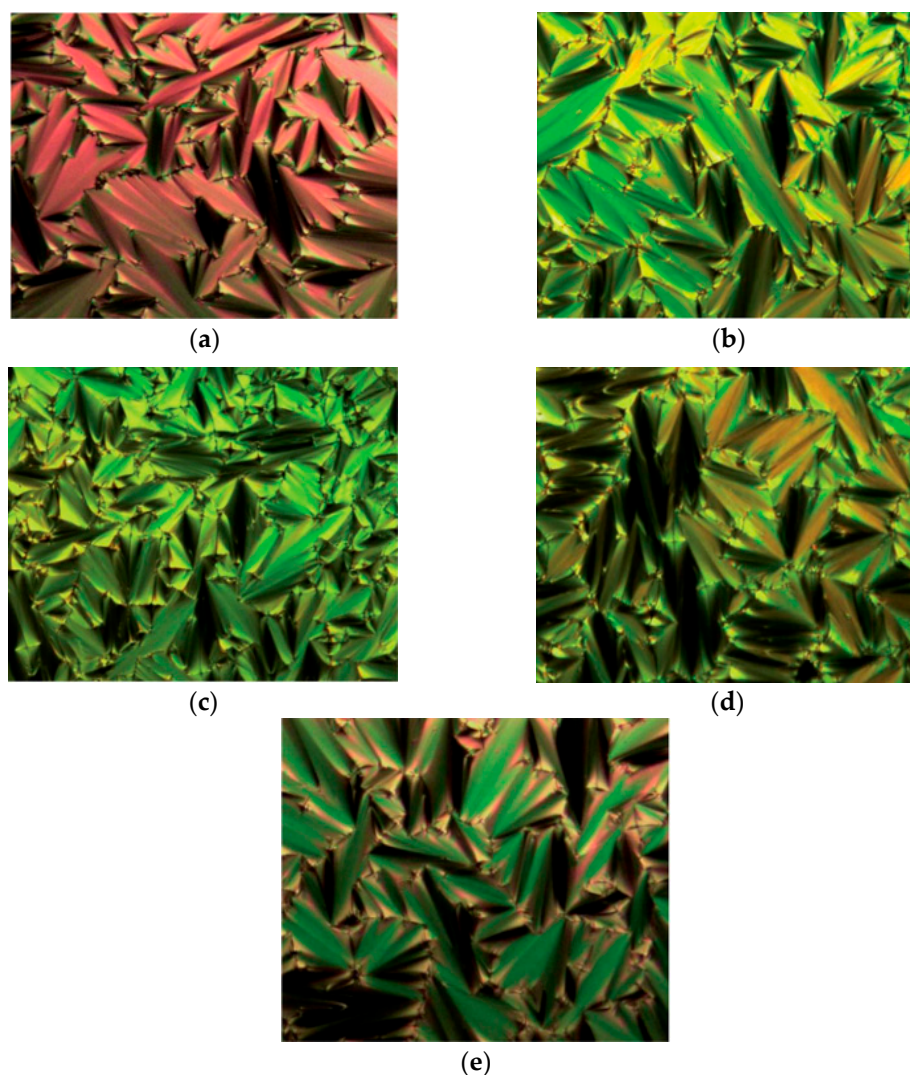


Figure 12. The optical photomicrograph of SmA phase for compound **11a–e**, (a) compound **11a** at 270.55 °C, (b) compound **11b** at 268.77 °C, (c) compound **11c** at 268.50 °C, (d) compound **11d** at 255.43 °C, and (e) compound **11e** at 247.78 °C. Reprinted/adapted with permission from Ref. [47]; published by Royal Society of Chemistry, 2020.

The DSC thermograms of compounds **11(a–e)** showed two curves for the transition from crystal to SmA and to the isotropic level. Both compounds in the heating cycle showed elevated melting and clearing temperatures. The melting rate was determined from the DSC data at 188.02, 177.09, 174.44, 171.44, and 168.58 °C, which correlates respectively to compounds **11(a–e)**. The compounds' melting and clearing temperature revealed a comparable trend in which the temperature declined as the number of alkyl chains increased.

As a reference, compound **c** was used for further review. The XRD diffractogram of **5c** can be seen in Figure 13. A single sharp peak at $2\theta = 1.19^\circ$ and a wide peak with a wide angle at $2\theta = 15\text{--}21^\circ$ were seen by the XRD diffractogram of compound **11c**, showing that the molecules support the smectic layered structure. The compound that typically showed the smectic liquid crystalline phase showed a sharp and high low-angle peak ($1^\circ > 2\theta > 4^\circ$) and a large peak in the XRD curve at $2\theta \approx 20^\circ$ [42]. The sharp peak showed the standard spaced layer structure, while the disordered packing of alkyl chains had a broad peak. The estimated d/L was 1.11 ($d \approx L$), equivalent to approximately 1. This phenomenon shows that monolayer structure is the SmA phase determined under POM. The side arms linked to the cyclotriphosphazene ring's phosphorus atoms were arranged three up and three down. These side arms conform perpendicular to the cyclotriphosphazene ring as

this form is appropriate for the smectic configuration due to the behaviour of homeotropic alignment.

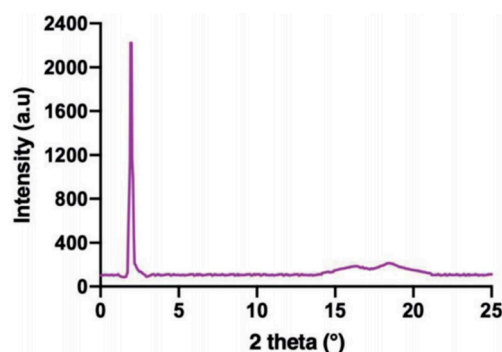


Figure 13. XRD diffractogram of compound **11c**. Reprinted/adapted with permission from Ref. [47]; published by Royal Society of Chemistry, 2020.

A molecule's skeleton configurations affect the properties of the liquid crystal. In order to exhibit liquid crystal mesophase, a compound must have a certain requirement. There is a profound impact on the existence of the terminal substituents or end groups in the mesogen molecule. The terminal group that extends the long molecular axis without increasing molecular diameter increases the mesophase thermal stability [53]. Many molecules consist of a single terminal alkyl chain exhibiting the behaviour of liquid crystals. This was shown when all the final compounds **11(a–e)** with the alkoxy chains at the terminal end saw the smectic A stage of both cooling and heating processes. The length of the side chain of the alkoxy displayed a greater effect on the shape of the mesophase. The liquid crystal activity with wider temperature ranges was caused by longer alkoxy chains and reduced melting temperatures. At the terminal end, all **11(f–j)** compounds with small substituents were considered to be non As a result, it is difficult to cause the development of the mesophase in the molecules. High melting temperature resulted in the presence of the amide linking unit and the mesophase cannot be detected for **11h** and **11i**. Because of the properties of the NH_2 , compound **11j** did not reveal any liquid crystals, leading to a decrease in mesophase formation.

The latest finding on the cyclotriphosphazene with Schiff base and azo linking units was reported by Jamain et al. (2021) [48]. In this study, all the compounds with alkoxy terminal group (**12a–e**) showed the texture of SmA and nematic phases. The existence of SmA was due to the lamellar packing in the molecules. This packing can induce high Van der Waal interactions between alkyl chains, which resulted in the nematic orientation not being favoured. However, the presence of an azo linking unit is able to stabilize these interactions by maintaining the linearity of the side arms. Moreover, the nematogenic character in compound **12i** was due to the strong dipole moment of the chlorine group.

3. Physical Properties

The combination of cyclotriphosphazene with Schiff base linkage is able to induce the physical properties of the compounds. The reported cyclotriphosphazene compounds containing different side arms are illustrated in Table 6.

Table 6. Cyclotriphosphazene compounds containing different side arms.

Structure of Compound	Terminal Group	Ref.
<p style="text-align: center;">Compounds 14a-c</p>	R = F (14a); Cl (14b); Br (14c)	[54]
<p style="text-align: center;">Compounds 15a-c</p>	R = -(15a); CH ₂ (15b); (15c)	[55]
<p style="text-align: center;">Compound 16</p>	-	[56]
<p style="text-align: center;">Compound 17a</p>	-	[57]

Table 6. Cont.

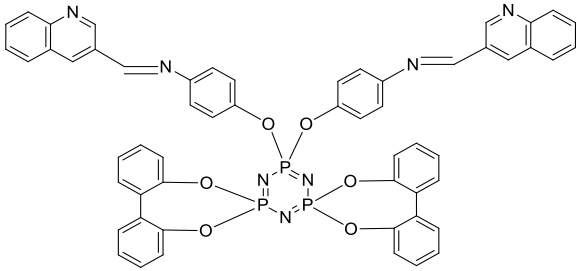
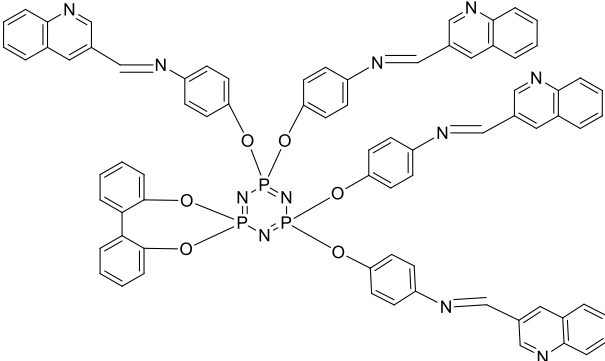
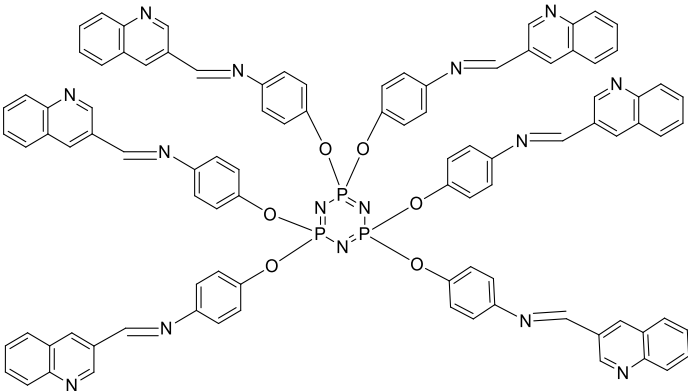
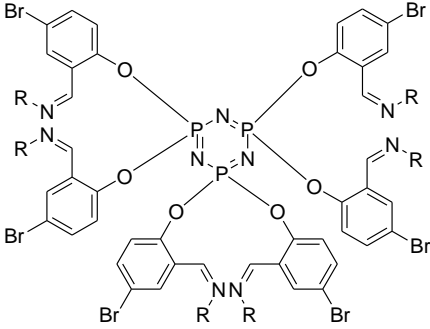
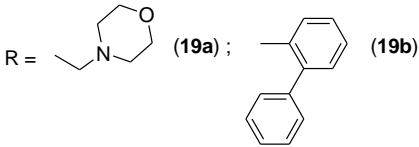
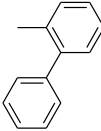
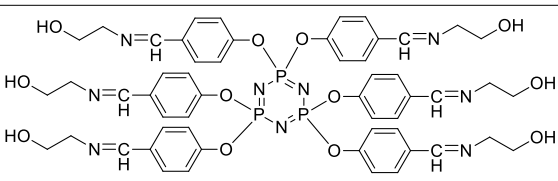
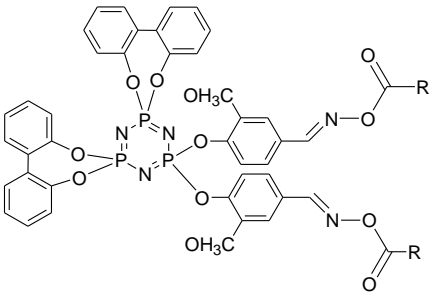
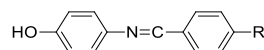
Structure of Compound	Terminal Group	Ref.
 <p>Compound 18a</p>	-	[58]
 <p>Compound 18b</p>	-	[58]
 <p>Compound 18c</p>	-	[58]
 <p>Compounds 19a–b</p>	 <p>R =  (19a);  (19b)</p>	[59]

Table 6. Cont.

Structure of Compound	Terminal Group	Ref.
 <p style="text-align: center;">Compound 20</p>	-	[60]
 <p style="text-align: center;">Compounds 21a–c</p>	<p>R =  (21a);  (21b);</p> <p> (21c)</p>	[61]

A study conducted by Dogan et al., in 2020 stated that a cyclotriphosphazene compound bearing an alternating phosphorus and nitrogen atom exhibits a typical thermal property [54]. The melting point of compounds **14(a–c)** was higher compared to the Schiff base compounds **13(a–c)**. The thermal stabilities of cyclotriphosphazene derivatives **14(a–c)** are higher compared to compounds **13(a–c)**. The onset decomposition temperature (T_{on}) and the maximum point of decomposition temperature (T_{dm}) values decreased from **14c**, **14b** and **14a**. Hence, the thermal stability of the compound was reduced in the same order. The main factor affecting this decline is the size of halogen group substitution on the Schiff base. As the size of the halogen atom increases, the decomposition cross-linking process decreases as well. The second factor explaining this phenomenon is the increase in bond dissociation energy from $C-Br < C-Cl < C-F$. The char yield of cyclotriphosphazene compounds **14(a–c)** is high due to the P–N skeleton and cross-linking process on decomposition. However, compounds **14(a–c)** does not show significant fluorescence properties as the $C=N$ isomerization is the main decay process of Schiff base excited states with an unbridged $C=N$ structure are usually non-fluorescence.



Compound	13a	13b	13c
R	F	Cl	Br

Compounds **15(a–c)** show good thermal stability since there is no significant weight loss detected up to 350 °C [55]. TGA curves suggest that there is a strong destabilization zone from 370–500 °C. Compound **15c** shows better thermal stability compared to the other compound as the decomposition of compound **15c** starts at 428 °C. It may be due to the presence of a chemically stable $S=(O)_2$ group located in the polymer backbone. Compound **15c** shows a distinctive weight loss curve between 449–610 °C and it is because of the loss of bulky $S=(O)_2$. The TGA curves suggest that the amount of char accumulated at 700 °C is noticeable between 42 to 36%, because of the partial scission and repolymerizing of cyclotriphosphazene rings followed by the increase in crosslinking density causing the formation of a thick char layer. This development of a thick char layer lessens the transmission of heat to the polymeric materials under it [62].

Stoke's shift value is the difference between the excitation and emission maximum. High Stoke's shift value is crucial for fluorescence and optical sensor studies. Compound **16** exhibits high Stoke's shift value of 123 nm due to the longer conjugated π system [56]. Compounds **17(a–b)** are the most fluorescence compound out of all the compounds studied [57]. Both compounds display an intense emission band at 745 nm and 753 nm, respectively and the largest Stoke's shift. The molecular structure of compound **17b** is shown in Figure 14.

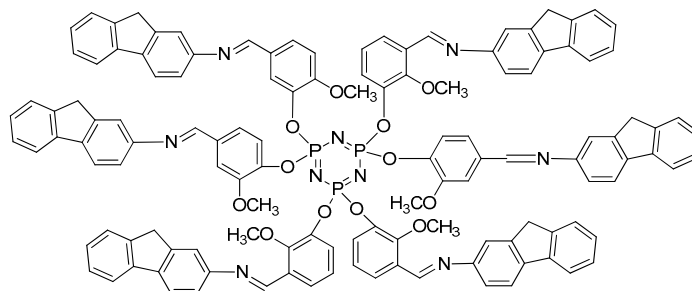


Figure 14. Molecular structure of compound **17b** [57].

Ibisoglu et al. studied those compounds **18(a–c)** are highly soluble in organic solvents such as THF, dichloromethane and ethanol, but have low solubility in n-hexane and water [58]. The UV-vis absorption curve shows that the absorption decreases linearly when the solution is diluted without any red/blue shift. The absence of the red/blue shift suggests that there is no inter/intramolecular interaction between the Schiff base ligand on the cyclotriphosphazene core. All compound studied showed no fluorescence properties, since Schiff base derivatives containing C=N structure does not show fluorescence properties. Even when the concentration of the compound decrease, the fluorescence intensities do not change, which indicates that the self-quenching effect does not exist within the attached fluorophore groups.

The absorption spectra of compounds **19(a–b)** display two strong bands ranging from 230 to 300 nm, this absorption might be due to the π - π^* transition of the cyclotriphosphazene bonded organic groups. All compounds **19(a–c)** emitted fluorescence peaks between 310–410 nm, observed from the fluorescence spectra. The largest fluorescence peak detected is 410 nm, emitted by compounds **19c** (Figure 15). All compounds **19(a–c)** are soluble in organic solvents such as chloroform, dichloromethane, and acetone [59].

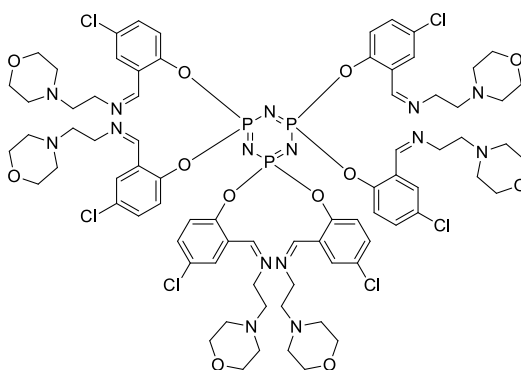


Figure 15. Molecular structure of compound **19c** [59].

Under high temperatures, compound H has a char-forming control. The residue char of compound **20** exceed 69.99 wt% at exactly 600 °C. This is due to a large amount of cyclotriphosphazene present in compound H along with the aromatic structure. In addition, at a higher temperature, crosslinking of azomethine occur which leads to less weight loss [60]. The study of the incorporation of FR-WPU/H5 film led to the reinforcement of tensile strength and Young's modulus. The rigid benzene ring unit in compound **20** enhances the

degree of physical cross-linking, causing the phase separation degree of FR-WPU/H5 film to increase. This will later improve the tensile strength and Young's modulus.

The dielectric constant of a compound reduces against increasing frequency. The constant became obvious at low-frequency values of 1–1000 Hz. One of the factors affecting the increase in the dielectric constant is the existence of polar groups within the structure of the compound. The carbonyl group bonded to the oxime-ester groups of compounds **21(a–c)** cause the dielectric constant to be high. Compound **21d** (Figure 16), an oxime-ester phosphazene compound bearing a thiophene group, displays higher conductivity than the rest of compound **21**. The dielectric constant and the alternating-current conductivity of compound **21d** are 7.87 and 3.41×10^{-6} , respectively. This is caused by the existence of polar groups and π electron conjugation such as the carbonyl group and the thiophene [61].

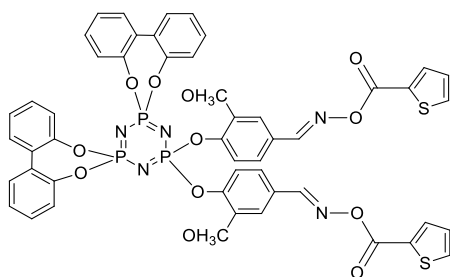


Figure 16. Molecular structure of compound **21d** [61].

4. Conclusions

This review shows there is an impact on the existence of the terminal substituents or end groups in the mesogenic molecule. There is no mesophase activity in some of the molecules with minor substituents. The thermal displacement disrupts the order of the liquid crystal phase when the temperature is too high, forcing the substance into the isotropic phase. If the temperature is too low, most of the liquid crystal becomes crystal. The development of new liquid crystalline compounds and the determination of the properties of these mesogenic molecules have gained significant interest. Although most of the synthesized liquid crystal molecules have shown a very similar structure, which defines their physical properties, the experimental data on the properties of mesogenous molecules are minimal. The existence of Schiff base linking units and cyclotriphosphazene impacted liquid crystal fields. Cyclotriphosphazene and its derivatives are good models for structure-activity research, and their multiarmed and rigid rings enable the discovery of new liquid crystalline molecules. Small structural changes can be done in order to explore the behaviour of this chemical, which has both organic and inorganic side chains. Moreover, the modification of cyclotriphosphazene core systems allows the introduction of a wide range of substituents and provides substituted cyclotriphosphazene derivatives with different chemical and physical properties, such as advanced liquid crystal devices and fire-retardant materials.

Author Contributions: Conceptualization, Z.J., M.Z.H.M. and A.N.A.A.; methodology, Z.J.; software, Z.J. and N.A.R.; validation, Z.J., A.N.A.A. and N.A.R.; formal analysis, Z.J. and N.A.R.; investigation, Z.J.; resources, Z.J.; data curation, Z.J. and A.N.A.A.; writing—original draft preparation, Z.J. and A.N.A.A.; writing—review and editing, Z.J., N.A.R. and M.Z.H.M.; visualization, Z.J. and A.N.A.A.; supervision, Z.J. and M.Z.H.M.; project administration, Z.J.; funding acquisition, Z.J. All authors have read and agreed to the published version of the manuscript.

Funding: This research was funded by Universiti Malaysia Sabah (UMS), grant numbers SBK0488-2021 and SPB0004-2020; and The APC was funded by Universiti Malaysia Sabah (UMS).

Institutional Review Board Statement: Not applicable.

Informed Consent Statement: Not applicable.

Data Availability Statement: Not applicable.

Acknowledgments: The authors would like to thank Universiti Malaysia Sabah (UMS) for its technical and financial support.

Conflicts of Interest: The authors declare no conflict of interest.

References

1. Lejček, L.; Glogarová, M.; Těšínská, E. Commemorative Plaque of Prof. Friedrich Reinitzer Installed in Prague. *Liq. Cryst. Today* **2017**, *26*, 66–68. [[CrossRef](#)]
2. Jamain, Z.; Habil, S.; Makmud, M.Z.H.; Khairuddean, M. Synthesis, structural and dielectric characteristics of liquid crystalline azo-based compounds with different terminal length. In Proceedings of the 2021 IEEE International Conference on the Properties and Applications of Dielectric Materials (ICPADM), Johor Bahru, Malaysia, 12–14 July 2021; pp. 49–52.
3. Srinivasa, H.T.; Palakshamurthy, B.S.; Devarajegowda, H.C.; Hariprasad, S. Synthesis, Characterization, Crystal Structure and Liquid Crystal Studies of Some Symmetric Naphthalene Derivative Molecules. *J. Mol. Struct.* **2018**, *1173*, 620–626. [[CrossRef](#)]
4. Raynes, P. Liquid Crystals—Second Edition, by S Chandrasekhar, Cambridge University Press, (1992), ISBN 0-521-41747-3 (HB), ISBN 0-521-42741-X (PB). *Liq. Cryst. Today* **1993**, *3*, 7. [[CrossRef](#)]
5. D'Errico, G.; Paduano, L. NMR of Liquid Crystals and Micellar Solutions. In *Nuclear Magnetic Resonance*; Royal Society of Chemistry: Cambridge, UK, 2010; pp. 424–455.
6. Dierking, I.; Al-Zangana, S. Lyotropic Liquid Crystal Phases from Anisotropic Nanomaterials. *Nanomaterials* **2017**, *7*, 305. [[CrossRef](#)] [[PubMed](#)]
7. Jamain, Z.; Khairuddean, M. Synthesis and Mesophase Behaviour of Benzylidene-Based Molecules Containing Two Azomethine Units. *J. Phys. Conf. Ser.* **2021**, *1882*, 012120. [[CrossRef](#)]
8. Shalaev, E.; Wu, K.; Shamblin, S.; Krzyzaniak, J.F.; Descamps, M. Crystalline Mesophases: Structure, Mobility, and Pharmaceutical Properties. *Adv. Drug Deliv. Rev.* **2016**, *100*, 194–211. [[CrossRef](#)]
9. Jamain, Z.; Khairuddean, M.; Saidin, S.A. Synthesis and Characterization of 1,4-Phenylenediamine Derivatives Containing Hydroxyl and Cyclotriphosphazene as Terminal Group. *J. Mol. Struct.* **2019**, *1186*, 293–302. [[CrossRef](#)]
10. Jamain, Z.; Omar, N.F.; Khairuddean, M. Synthesis and Determination of Thermotropic Liquid Crystalline Behavior of Cinnamaldehyde-Based Molecules with Two Schiff Base Linking Units. *Molecules* **2020**, *25*, 3780. [[CrossRef](#)]
11. Singh, S.; Dunmur, D. *Liquid Crystals: Fundamentals*; World Scientific Publishing Co. Pte. Ltd.: London, UK, 2002; pp. 94–108.
12. Kitzerow, H.S.; Bahr, C. *Chirality in Liquid Crystals*; Springer: Berlin/Heidelberg, Germany, 2001.
13. Razali, N.; Jamain, Z. Liquid Crystals Investigation Behavior on Azo-Based Compounds: A Review. *Polymers* **2021**, *13*, 3462. [[CrossRef](#)]
14. Jamain, Z.; Khairuddean, M.; Loh, M.L.; Manaff, N.L.A.; Makmud, M.Z.H. Synthesis and Characterization of Hexasubstituted Cyclotriphosphazene Derivatives with Azo Linking Units. *Malays. J. Chem.* **2020**, *22*, 125–140.
15. Andrienko, D. Introduction to Liquid Crystals. *J. Mol. Liq.* **2018**, *267*, 520–541. [[CrossRef](#)]
16. Safinya, C.R.; Varady, W.A. Calamitic Liquid Crystals-Nematic and Smectic Mesophases. *Liq. Cryst.* **1986**, *57*, 43–77.
17. Lehn, J.-M. Introduction to Liquid Crystal. In *Supramolecular Chemistry*; Wiley-VCH: Weinheim, Germany, 1995; pp. 177–219.
18. Bag, S.; Maingi, V.; Maiti, P.K.; Yelk, J.; Glaser, M.A.; Walba, D.M.; Clark, N.A. Molecular Structure of the Discotic Liquid Crystalline Phase of Hexa-Peri-Hexabenzocoronene/Oligothiophene Hybrid and Their Charge Transport Properties. *J. Chem. Phys.* **2015**, *143*, 144505. [[CrossRef](#)] [[PubMed](#)]
19. Panchatcharam, U.C. Ordering Properties of Oligomeric Columnar Discotic Liquid Crystals. Ph.D. Thesis, Wageningen University, Wageningen, The Netherlands, 2015.
20. Nitschke, P.; Jarzabek, B.; Vasylieva, M.; Honisz, D.; Małeck, J.G.; Musioł, M.; Janeczek, H.; Chaber, P. Influence of Chemical Structure on Thermal, Optical and Electrochemical Properties of Conjugated Azomethines. *Synth. Met.* **2021**, *273*, 116689. [[CrossRef](#)]
21. Chong, Y.T.; Muhamad Sari, N.; Ha, S.T.; Sheikh, M.R.K. New Homologues Series of Heterocyclic Schiff Base Ester: Synthesis and Characterization. *Adv. Phys. Chem.* **2016**, *2016*, 7647695. [[CrossRef](#)]
22. Kim, Y.H.; Yoon, D.K.; Jeong, H.S.; Lavrentovich, O.D.; Jung, H.T. Smectic Liquid Crystal Defects for Self-Assembling of Building Blocks and Their Lithographic Applications. *Adv. Funct. Mater.* **2011**, *21*, 610–627. [[CrossRef](#)]
23. Kiliç, M.; Çinar, Z. Structures and Mesomorphic Properties of Cyano-Containing Calamitic Liquid Crystal Molecules. *J. Mol. Struct. THEOCHEM* **2007**, *808*, 53–61. [[CrossRef](#)]
24. Kajal, A.; Bala, S.; Kamboj, S.; Sharma, N.; Saini, V. Schiff Bases: A Versatile Pharmacophore. *J. Catal.* **2013**, *2013*, 893512. [[CrossRef](#)]
25. Ha, S.T.; Lee, T.L.; Yeap, G.Y.; Ito, M.M.; Saito, A.; Watanabe, M. Mesomorphic Behavior of New Azomethine Liquid Crystals Having Terminal Iodo Group. *Chin. Chem. Lett.* **2011**, *22*, 260–263. [[CrossRef](#)]
26. Ha, S.T.; Lee, T.L.; Lee, S.L.; Yeap, G.Y.; Win, Y.F.; Ong, S.T. Mesomorphic Behaviour of New Azomethine Liquid Crystals Having Terminal Bromo Substituent. *Chin. Chem. Lett.* **2012**, *23*, 177–180. [[CrossRef](#)]
27. Kostromin, S.; Bronnikov, S.; Perju, E.; Cozan, V. Kinetics of the Ordered Phase Growth across the Isotropic-Nematic Phase Transition in Liquid Crystal Azomethine Polymers during Cooling. *J. Macromol. Sci. Part B Phys.* **2012**, *51*, 2105–2112. [[CrossRef](#)]

28. Nafee, S.S.; Hagar, M.; Ahmed, H.A.; Alhaddad, O.A.; El-Shishtawy, R.M.; Raffah, B.M. New Two Rings Schiff Base Liquid Crystals; Ball Mill Synthesis, Mesomorphic, Hammett and DFT Studies. *J. Mol. Liq.* **2020**, *299*, 112161. [[CrossRef](#)]
29. Hagar, M.; Ahmed, H.A.; Nafee, S.S.; El-Shishtawy, R.M.; Raffah, B.M. The Synthesis of New Thermal Stable Schiff Base/Ester Liquid Crystals: A Computational, Mesomorphic, and Optical Study. *Molecules* **2019**, *24*, 3032. [[CrossRef](#)]
30. Demus, D.; Ritcher, L. Textures of Liquid Crystals. In *Crystal Research & Technology*; VEB Deutscher Verlag für Grundstoffindustrie: Leipzig, Germany, 1981; Volume 16, p. 527.
31. Dierking, I. The Fluid Smectic Phase. In *Textures of Liquid Crystals*; Wiley-VCH Verlag GmbH & Co. KGaA: Weinheim, Germany, 2003; pp. 91–122, ISBN 9783527602056.
32. Demus, D.; Goodby, J.; Gray, G.W.; Spiess, H.-W.; Vill, V.; Wiley-Vch, W. Physical Properties of Liquid Crystals. Wiley-VCH: Weinheim, Germany, 1990.
33. Berdagué, P.; Bayle, J.P.; Ho, M.-S.; Fung, B.M. New Laterally Aromatic Branched Liquid Crystal Materials with Large Nematic Ranges. *Liq. Cryst.* **1993**, *14*, 667–674. [[CrossRef](#)]
34. Naser, J.; Himdan, T.; Al-Dujaili, A. Synthesis and Characterization of Schiff-Bases Liquid Crystalline Containing 1,3,4-Oxadiazole Rings. *J. Int. Acad. Res. Multidiscip.* **2014**, *2*, 415–426.
35. Naoum, M.M.; Metwally, N.H.; Abd eltawab, M.M.; Ahmed, H.A. Polarity and Steric Effect of the Lateral Substituent on the Mesophase Behaviour of Some Newly Prepared Liquid Crystals. *Liq. Cryst.* **2015**, *42*, 1351–1369. [[CrossRef](#)]
36. Hagar, M.; Ahmed, H.; Hussien, T.; Alnoman, R. Mesophase Behavior and DFT Conformational Analysis of New Symmetrical Diester Chalcone Liquid Crystals. *J. Mol. Liq.* **2019**, *285*, 96–105. [[CrossRef](#)]
37. Jamain, Z.; Khairuddean, M.; Nabilah Zulbaharen, N.; Keen Chung, T. Synthesis, Characterization and Determination of Mesophase Transition of Azo-Azomethine Derivatives with Different Terminal Chain Lengths. *Malays. J. Chem.* **2019**, *21*, 73–85.
38. Wahl, H.; Haynes, D.A.; le Roex, T. Lack of Co-Crystal Formation with Cyclotriphosphazenes: A Cautionary Tale. *S. Afr. J. Chem.* **2016**, *69*, 35–43. [[CrossRef](#)]
39. Usri, S.N.K.; Jamain, Z.; Makmud, M.Z.H. A Review on Synthesis, Structural, Flame Retardancy and Dielectric Properties of Hexasubstituted Cyclotriphosphazene. *Polymers* **2021**, *13*, 2916. [[CrossRef](#)]
40. Patel, R.B.; Doshi, A.V. Synthesis and Study of New Ester Homologous Series: Ethyl-p-(p/-n/Alkoxy Cinnamoloxy)Cinnamtes. *Der Pharma Chem.* **2011**, *3*, 557–565.
41. Sharma, V.S.; Patel, R.B. Effect of Alkyl Chain in the Terminal Ester Group on Mesomorphic Properties of New Rod like Homologous Series: Synthesis and Characterization. *Mol. Cryst. Liq. Cryst.* **2017**, *643*, 62–75. [[CrossRef](#)]
42. Gulbas, H.E.; Coskun, D.G.; Gursel, Y.H.; Bilgin-Eran, B. Synthesis, Characterization and Mesomorphic Properties of Side Chain Liquid Crystalline Oligomer Having Schiff Base Type Mesogenic Group. *Adv. Mater. Lett.* **2014**, *5*, 333–338. [[CrossRef](#)]
43. Ha, S.-T.; Lee, T.-L. Synthesis and Mesomorphic Properties of New Fluorinated Schiff Base Liquid Crystals. *ISRN Mater. Sci.* **2014**, *2014*, 904657. [[CrossRef](#)]
44. Barberá, J.; Jiménez, J.; Laguna, A.; Oriol, L.; Pérez, S.; Serrano, J.L. Cyclotriphosphazene as a Dendritic Core for the Preparation of Columnar Supermolecular Liquid Crystals. *Chem. Mater.* **2006**, *18*, 5437–5445. [[CrossRef](#)]
45. Bao, R.; Pan, M.; Qiu, J.J.; Liu, C.M. Synthesis and Characterization of Six-Arm Star-Shaped Liquid Crystalline Cyclotriphosphazenes. *Chin. Chem. Lett.* **2010**, *21*, 682–685. [[CrossRef](#)]
46. Jamain, Z.; Khairuddean, M.; Guan-Seng, T. Synthesis of New Star-Shaped Liquid Crystalline Cyclotriphosphazene Derivatives with Fire Retardancy Bearing Amide-Azo and Azo-Azo Linking Units. *Int. J. Mol. Sci.* **2020**, *21*, 4267. [[CrossRef](#)]
47. Jamain, Z.; Khairuddean, M.; Guan-Seng, T. Synthesis of Novel Liquid Crystalline and Fire Retardant Molecules Based on Six-Armed Cyclotriphosphazene Core Containing Schiff Base and Amide Linking Units. *RSC Adv.* **2020**, *10*, 28918–28934. [[CrossRef](#)]
48. Jamain, Z.; Khairuddean, M.; Guan-Seng, T.; Rahman, A.B.A. Synthesis, Characterisation and Mesophase Transition of Hexasubstituted Cyclotriphosphazene Molecules with Schiff Base and Azo Linking Units and Determination of Their Fire Retardant Properties. *Macromol. Res.* **2021**, *29*, 331–341. [[CrossRef](#)]
49. Jeong, M.J.; Park, J.H.; Lee, C.; Chang, J.Y. Discotic Liquid Crystalline Hydrazone Compounds: Synthesis and Mesomorphic Properties. *Org. Lett.* **2006**, *8*, 2221–2224. [[CrossRef](#)]
50. Li, Q.; Huang, R.; Xiong, S.; Xie, X. Synthesis, Mesophase Behaviour and Design Principles for Discotic Liquid Crystals of Phenyl Ethynylene Macrocycles with in-Traannular Flexible Chains. *Liq. Cryst.* **2012**, *39*, 249–258. [[CrossRef](#)]
51. Nagaveni, N.G.; Roy, A.; Prasad, V. Achiral Bent-Core Azo Compounds: Effect of Different Types of Linkage Groups and Their Direction of Linking on Liquid Crystalline Properties. *J. Mater. Chem.* **2012**, *22*, 8948–8959. [[CrossRef](#)]
52. Selvarasu, C.; Kannan, P. Effect of Azo and Ester Linkages on Rod Shaped Schiff Base Liquid Crystals and Their Photophysical Investigations. *J. Mol. Struct.* **2016**, *1125*, 234–240. [[CrossRef](#)]
53. Thaker, B.T.; Patel, P.H.; Vansadiya, A.D.; Kanojiya, J.B. Substitution Effects on the Liquid Crystalline Properties of Thermotropic Liquid Crystals Containing Schiff Base Chalcone Linkages. *Mole. Cryst. Liq. Cryst.* **2009**, *515*, 135–147. [[CrossRef](#)]
54. Doğan, S.; Tümay, S.O.; Mutlu Balci, C.; YeşilLot, S.; Besli, S. Synthesis of New Cyclotriphosphazene Derivatives Bearing Schiff Bases and Their Thermal and Absorbance Properties. *Turk. J. Chem.* **2020**, *44*, 31–47. [[CrossRef](#)] [[PubMed](#)]
55. Al-Shukri, S.M.; Mahmood, A.T.; al Hanbali, O.A. Spiro-Cyclotriphosphazene with Three Functional End Groups: Synthesis and Structural Characterization of New Polycyclotriphosphazenes with Schiff-Base Groups. *Polimery* **2021**, *66*, 341–349. [[CrossRef](#)]

56. Aslan, F.; Demirpençe, Z.; Tatsız, R.; Turkmen, H.; Oztürk, A.I.; Arslan, M. The Synthesis, Characterization and Photophysical Properties of Some New Cyclotriphosphazene Derivatives Bearing Schiff Base. *Z. Anorg. Allg. Chem.* **2008**, *634*, 1140–1144. [[CrossRef](#)]
57. Aslan, F.; Öztürk, A.İ.; Söylemez, B. Synthesis of Fluorescence Organocyclotriphosphazene Derivatives Having Functional Groups Such as Formyl, Schiff Base and Both Formyl and Schiff Base without Using Ar or N₂ Atmosphere. *J. Mol. Struct.* **2017**, *1137*, 387–395. [[CrossRef](#)]
58. İbişoğlu, H.; Ün, Ş.Ş.; Erdemir, E.; Tümay, S.O. Synthesis, Characterization, and Photophysical Properties of Cyclotriphosphazenes Containing Quinoline-4-Aldehyde-p-Oxyanil Moieties. *Phosphorus Sulfur Silicon Relat. Elem.* **2021**, *196*, 760–768. [[CrossRef](#)]
59. Öztürk, A.İ.; Aslan, F.; Al, M. Synthesis, Characterization, and Spectroscopic Properties of Hexa(4-Bromo-2-Formyl-Phenoxy)Cyclotriphosphazene and Hexa(4-Chloro-2-Formyl-Phenoxy)Cyclotriphosphazene and Fully Substituted Cyclotriphosphazene Derivatives Bearing a Schiff Base at Room Temperature. *Phosphorus Sulfur Silicon Relat. Elem.* **2013**, *188*, 585–595.
60. Wang, H.; Du, X.; Wang, S.; Du, Z.; Wang, H.; Cheng, X. Improving the Flame Retardancy of Waterborne Polyurethanes Based on the Synergistic Effect of P-N Flame Retardants and a Schiff Base. *RSC Adv.* **2020**, *10*, 12078–12088. [[CrossRef](#)] [[PubMed](#)]
61. Koran, K.; Ozen, F.; Biryani, F.; Görgülü, A.O. Synthesis, Structural Characterization, and Dielectric Behavior of New Oxime-Cyclotriphosphazene Derivatives. *J. Mol. Struct.* **2015**, *1105*, 135–141. [[CrossRef](#)]
62. Jin, W.; Yuan, L.; Liang, G.; Gu, A. Multifunctional Cyclotriphosphazene/Hexagonal Boron Nitride Hybrids and Their Flame Retarding Bismaleimide Resins with High Thermal Conductivity and Thermal Stability. *ACS Appl. Mater. Interfaces* **2014**, *6*, 14931–14944. [[CrossRef](#)] [[PubMed](#)]